Solar Energy Materials & Solar Cells ∎ (∎∎∎∎) ∎∎∎–∎∎∎

Contents lists available at ScienceDirect

Solar Energy Materials & Solar Cells

journal homepage: www.elsevier.com/locate/solmat

Life cycle assessment of dynamic building integrated photovoltaics

P. Jayathissa [a,*,1], M. Jansen [a,1], N. Heeren [b], Z. Nagy [a], A. Schlueter [a]

[a] Architecture and Building Systems, Institute of Technology in Architecture, Department of Architecture, ETH Zurich, Switzerland
[b] Ecological System Design, Institute of Environmental Engineering, ETH Zurich, Switzerland

ARTICLE INFO

Article history:
Received 30 November 2015
Received in revised form
28 March 2016
Accepted 10 April 2016

Keywords:
Dynamic photovoltaics
Life cycle analysis
Multi functional envelope
BIPV
Adaptive shading

ABSTRACT

We assess the environmental impact of a dynamic, adaptive, building integrated photovoltaic (BIPV) systems. Such systems combine the benefits of adaptive shading with facade integrated solar tracking, thus reducing the building energy demand, and simultaneously generating electricity on-site. The inventory for the life cycle assessment (LCA) was acquired using production data, and Energy Plus simulations to calculate the building energy demand. The impact assessment was conducted according to ISO 14040 and ISO 14044 standards using the Eco-invent database and openLCA as an analysis tool. The embodied environmental impact of the dynamic BIPV solution is higher than a static alternative due to the added control system, electronics, actuators, and additional supporting structure, resulting in higher life cycle impacts. However when accounting for the systems multi-functionality aspect, i.e. savings through adaptive shading to the building's heating, cooling and lighting loads, the embodied environmental impact can be offset, making the ASF an interesting alternative for BIPV. We also conduct a sensitivity analysis to investigate modifications to the actuator type, control system, and location and find that none of the investigated parameters overturn the key findings. The analysis ultimately enables us to provide design recommendations for future dynamic BIPV installations.

1. Introduction

Buildings are at the heart of society and currently account for 32% of global final energy consumption and 19% of energy related greenhouse gas emissions [1]. Nevertheless the building sector has a 50–90% emission reduction potential using existing technologies, and widespread implementation could see energy use in buildings stabilise or even fall by 2050 [1]. Within this strategy, building integrated photovoltaics (BIPV) has the potential of providing a substantial segment of a building's energy needs [2]. Even the photovoltaic (PV) industry has identified BIPV as one of the four key factors for the future success of PV [3].

Recent developments regarding efficiency and costs of thin film BIPV technologies, in particular, CIGS, have brought new design possibilities [4–7]. Their lightweight nature and customisable shapes allow for easier and more aesthetically pleasing integration into the building envelope. In addition, less power is required to actuate them, thus facilitating the development of dynamic envelope elements due to their reduced weight [8].

Dynamic building envelopes have gained interest in recent years because they can save energy by controlling direct and indirect radiation into the building, while still responding to the desires of the user [9]. This mediation of solar insolation can offer a reduction in heating/cooling loads and an improvement of daylight distribution as seen in Fig. 1 [8]. Interestingly the structure and mechanics required for dynamic envelopes couples seamlessly with the structure and mechanics required for facade integrated PV solar tracking. The use of light weight PV as an adaptive envelope material enables it to also benefit from on-site energy production. Furthermore, it provides a new way of aesthetically integrating PV panels onto buildings. The balance of electricity production and adaptive shading can in some cases offset the entire energy demand of an office space behind the envelope [10]. We have proposed one possible combination of these technologies as an Adaptive Solar Facade (ASF) [11]. An example of an ASF can be seen in Fig. 2.

The design of an ASF comes at an added cost. The additional electronics, actuators, and supporting structure adds further embodied CO_2 to the product. It is therefore important to conduct a life cycle impact assessment (LCA) to analyse whether the life cycle environmental impacts are favourable, compared to a more classic system. It is also important to see how variations in design can alter the green house gas (GHG) reduction potential of the technology. Aspects such as the chosen actuator, control system,

* Corresponding author.
E-mail addresses: jayathissa@arch.ethz.ch (P. Jayathissa), m.jansen@student.ethz.ch (M. Jansen), heeren@ifu.baug.ethz.ch (N. Heeren), nagy@arch.ethz.ch (Z. Nagy), schlueter@arch.ethz.ch (A. Schlueter).
[1] Equally contributing first authors.

http://dx.doi.org/10.1016/j.solmat.2016.04.017
0927-0248/

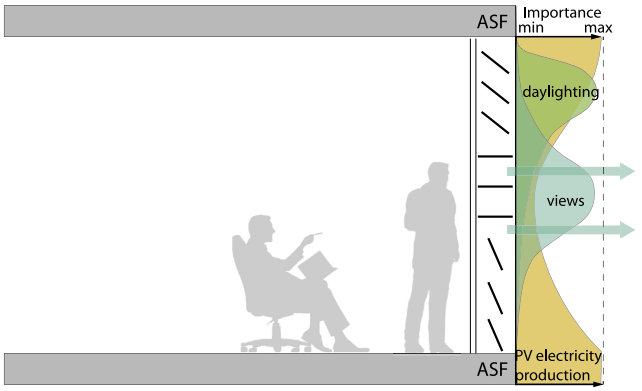

Fig. 1. The facade acting as a mediator between the interior and exterior environment, while fulfilling various functions [11].

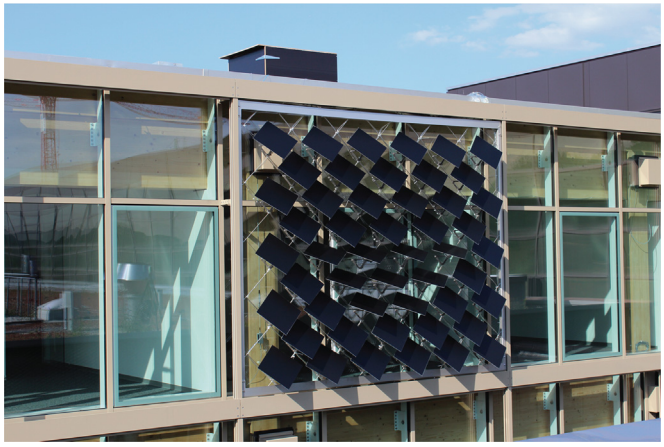

Fig. 2. An example of an ASF constructed at the House of Natural Resources [11].

and location of operation can have an impact on environmental performance.

The state of the art literature assesses existing photovoltaic technologies [12–14], and the balance of systems (BOS) which includes all other components of a photovoltaic system [15]. This has not, however, been expanded to dynamic BIPV systems, and in particular, systems that combine the benefits of adaptive shading and electricity production.

In this paper, we investigate the environmental performance of an ASF and compare it to existing static photovoltaic systems. We also investigate (1) a system expansion including the heating ventilation and air conditioning (HVAC) savings through adaptive shading, (2) design variations of the ASF, (3) the operational emissions of a building, with and without an ASF, and (4) the sensitivity of the LCA to its location and design.

The remainder of the paper is organised as follows. The following section introduces the ASF and the used LCA methodology. In Section 3, we present the results of the LCA analysis. Section 4 discusses the results and provides design guidelines. Section 5 concludes the paper.

2. Methodology

In this section, we detail the inventory, Energy Plus simulation methodology, important assumptions, and the LCA evaluation method. The assessment considers the environmental impacts of the production, operation, and disposal of an ASF. We assume a lifetime of 20 years based on the product warranty of the PV panels. The impact assessment is performed according to the ISO 14040 and ISO 14044, and is performed in four stages: (1) Goal and Scope Definition, (2) Inventory Analysis, (3) Impact Assessment, and (4) Interpretation [16].

1. *Goal and scope definition*: This paper primarily assesses carbon emission reductions therefore the global warming potential (GWP) impact category is primarily assessed. The assessment also looks at six other major ReCiPe midpoint indicators: terrestrial acidification potential (TAP), freshwater eutrophication potential (FEP), human toxicity potential (HTP), metal depletion potential (MDP), and photochemical oxidant formation potential (POFP). These categories are most relevant to the technology and most widely used in existing literature [17]. The functional unit is the electrical power production of the system in kWh.
   The scope of the assessment, respectively the system boundary, is summarised in Fig. 4. We analyse the manufacture, dynamic actuation, maintenance, and disposal of the solar facade. The scope comprises of a cradle-to-grave approach, where transport to and from site is taken into account. In order to account for the multi-functionality aspect of the ASF (i.e. electricity production and shading benefit), we carry out a sensitivity analysis and expand the system boundary including operational energy savings through adaptive shading. As the life cycle inventory (LCI) background database we use Ecoinvent v3.1 [18] with the cut-off system model.[2] That means impacts are allocated to the primary use of the product and it receives no credit for the provision of recycled material. Once a product is disposed or recycled, it leaves the system boundary and the recycled product comes burden-free.
2. *Inventory analysis*: The Ecoinvent v3.1 database is used as the main LCA database [18]. A detailed description of the inventory is found in Sections 2.1 and 2.2.
3. *Impact assessment*: The assessment is based on the IPCC 2007 methodology [19]. The GWP assessment is performed using the OpenLCA assessment tool [20]. In the assessment, we also compare the emission factor (EF) of an ASF with other PV systems. The emission factor is expressed as

$$EF = \frac{GWP}{G} \quad \left[\frac{\mathrm{kgCO_2-eq}}{\mathrm{kWh}}\right] \qquad (1)$$

   where (G) is the electricity production in (kWh).
4. *Interpretation*: The results of the LCA analysis (not including shading effects) are compared with other facade integrated PV technologies. We then perform a system expansion to also include the effects of adaptive shading to the system. Finally a sensitivity analysis is conducted which is further described in Section 2.3.

2.1. Embodied life cycle inventory

The mechanical components of an ASF can be broken into four parts: a PV panel, actuator, cantilever, and a cable net supporting structure. The PV panel, actuator and cantilever combine to form a dynamic PV module, which is then mounted on a cable net supporting structure. An exploded view of these components can be seen in Fig. 3. There are also additional electronics which exists off

[2] http://www.ecoinvent.org/database/system-models-in-ecoinvent-3/cut-off-system-model/allocation-cut-off-by-classification.html – *Accessed*: 8.2.2016.

Please cite this article as: P. Jayathissa, et al., Life cycle assessment of dynamic building integrated photovoltaics, Solar Energy Materials and Solar Cells (2016), http://dx.doi.org/10.1016/j.solmat.2016.04.017

the facade in a separate control box. These five components along with the assembly, are the main product systems in the manufacture of an ASF as seen in Fig. 4. The inventory quantities are given in specific mass quantity (SMQ), which is the mass in kg of the specific materials.

PV panel: Weight is the primary restriction when selecting a PV panel. Any technology that requires glass encapsulation or a heavy substructure can therefore not be used. The technology also needs to be on the market with high module efficiency. CIGS PV panels were selected as the thin film panel of choice due to its high efficiency, low cost, and ability to be deposited on a polymer or aluminium substrate [21] (Table 1).

Actuator: Traditionally photovoltaic actuation is done through the use of servo motors. Servo motors however become a limiting factor for adaptive facades due to their high upfront costs, and instability in heavy winds. Soft robotic actuators on the other hand are cheaper and more resilient to harsh environmental conditions [22]. The soft robotic actuators however are still in development and have an estimated lifetime of 5 years. They will therefore require three rounds of maintenance during the lifetime of the ASF. For the purpose of this assessment we will run a sensitivity analysis on the use of servo motors and soft robotic actuators (Table 2).

Cantilever: The cantilever is a steel connection point between the PV panel and the supporting structure (Table 3).

Supporting structure: The supporting structure is the connection point between the array of photovoltaic modules and the building itself. Many different designs are possible, however, we will base our analysis of an existing adaptive solar facade [11]. This design consists of a steel

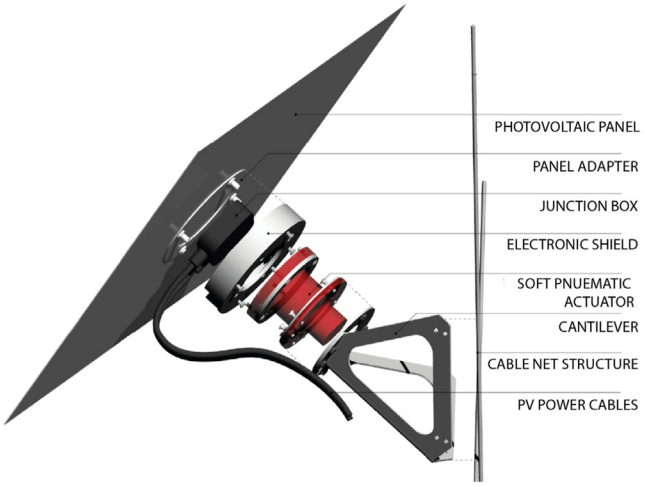

Fig. 3. Exploded view of an ASF module mounted on a cable net supporting structure.

Table 1
Inventory in specific mass quantity (SMQ) of the top five input flows to the PV manufacturing process.

Material description	SMQ (/m^2facade)
CIGS PV film	0.569 m^2_{PV}
Aluminum sheet	1.593 kg
Chromium steel panel adapter	1.422 kg
Polyethylene for junction box	0.036 kg
Diode, glass for junction box	0.011 kg

Table 2
Inventory of four main input flows to the soft robotic actuator manufacturing process.

Material description	SMQ (kg/m^2_{facade})
Chromium steel rings	1.0665
Electronics, for control, 2-2way valves	0.0130
Silicone chambers	0.8887
Polyurethane tubes	0.0933
Air compressor, screw type, 0.75 kW	1.7281

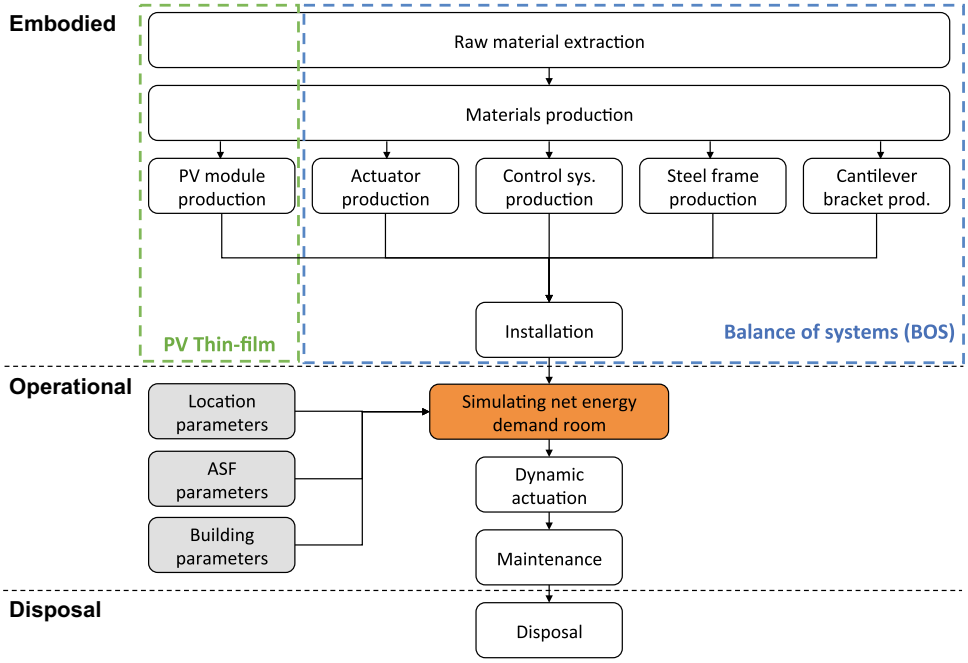

Fig. 4. Breakdown of the ASF into five embodied product components, installation, operation, and disposal.

Please cite this article as: P. Jayathissa, et al., Life cycle assessment of dynamic building integrated photovoltaics, Solar Energy Materials and Solar Cells (2016), http://dx.doi.org/10.1016/j.solmat.2016.04.017

cable-net that spans a steel supporting frame. The steel frame is then mounted on the building facade (Table 4).

Control system and electronics: The control system is required for the actuation of panels and the regulation of photovoltaic electricity production (Table 5).

Assembly: There are many assembly options available. From past experience, an installation of an equivalent ASF required a hydraulic hoist which was in operation for eight hours [10] (Table 6).

2.2. Operational life cycle inventory

The operational inventory is categorised as (1) energy consumption of an office room, (2) electricity consumption through dynamic actuation, and (3) maintenance.

Building energy consumption: An adaptive shading system, when mounted over a glazed facade, has an impact on the energy consumption of the building. More specifically, it has an impact on the heating cooling and lighting loads as described in Section 1. Previously conducted simulations compared three scenarios: (1) facade with no shading, (2) a facade with a static shading system, optimally angled at 45° to the horizontal axis, and (3) an adaptive solar facade [10]. The simulation was conducted on a south facing office room. The room, 7.0 m in length, 4.9 m wide and 3.1 m high, was modeled using Rhinoceros 3D CAD Package [23]. Grasshopper [24] was used to model the orientation of each photovoltaic panel. The geometrical input is imported to Energy Plus [25] through the DIVA [26] interface. A single zone thermal analysis was conducted for each possible geometrical configuration of the ASF for each hour of the year. The results were then post processed in MATLAB [27].

The simulations show a total energy saving of 25% compared to static panels at 45° and 56% compared to a case with no facade shading [10]. These results are summarised in Fig. 5. This data is used to perform our previously described sensitivity analysis which also accounts for HVAC energy savings through adaptive shading.

Dynamic actuation: The energy required for actuation is also taken into account. It takes 0.31 Wh to fully open a single actuator. Based on the assumption of four full openings and closings per day per actuator, we approximate the combined energy requirement to be 489 kWh in its 20 year lifetime.

Maintenance: Soft robotic actuators currently have a lifetime of 5 years, and therefore will need to be replaced three times during the 20 year lifetime of an ASF. No other maintenance efforts are considered for the assessment of 20 years (Table 7).

Table 3
Inventory of main input flows to the cantilever manufacturing process.

Material description	SMQ (kg/m^2_{facade})
Chromium steel bracket	1.4220
Chromium steel fixing clamp	0.0284

Table 4
Inventory of the four main input flows to the manufacturing process of the supporting structure.

Material description	SMQ (kg/m^2_{facade})
Chromium steel frame	6.9928
Chromium steel swaged external thread	0.2897
Chromium steel wire rope WC	0.1593

Table 5
Inventory of the four main input flows to the manufacturing process of the control system.

Material description	SMQ (kg/m^2_{facade})
Inverter 1.25 kW	0.6090
PV cable	0.256
Control electronics	0.0516

Table 6
Inventory of main input flows to the assembly process.

Material description	SMQ
Hoist, diesel <18.64 kW, idling	0.5267 h/m^2_{facade}

2.3. Sensitivity analysis

In order to evaluate the impact of varying parameters on the LCA, we performed a sensitivity analysis on the following assumptions:

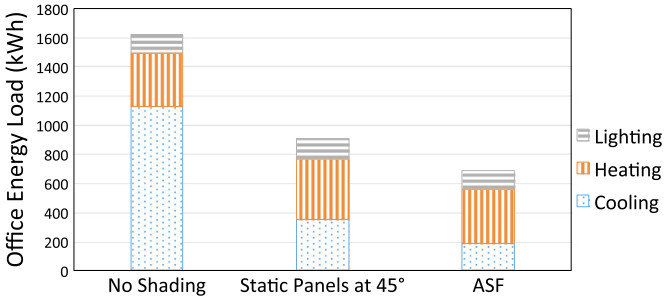

Fig. 5. Breakdown of operational energy consumption for a system in Frankfurt am Main with (a) no shading, (b) with louvers at 45° and (c) with an ASF – not including onsite electricity production.

Table 7
Summary of main assumptions for the calculation of operational emissions.

Building settings	
Office envelope	Roof: adiabatic
	Floor: adiabatic
	Walls: adiabatic
	Window: double glazed ($e=0.2$) 3 mm/13 mm air
Thermal set points	Heating: 22 °C
	Cooling: 26 °C
Building system	Hydronic heating: COP=4
	Hydronic cooling: COP=3
Lighting control	Lighting load: 11.8 W/m^2
	Lighting control: 300 lx threshold
Occupancy	Office: weekdays from 8:00 to 18:00
	People set point: 0.1 persons/m^2
	Infiltration: 0.5 air changes per hour
Location assumptions	
Weather file	Frankfurt am Main, Germany (106370IWEC)
Electricity mix	Germany (DE) [28]
Average solar radiation	855 kWh/m^2/year
Maintenance	
Actuator changes	Every 5 years
ASF assumptions	
Full openings and closings	4 per day

Please cite this article as: P. Jayathissa, et al., Life cycle assessment of dynamic building integrated photovoltaics, Solar Energy Materials and Solar Cells (2016), http://dx.doi.org/10.1016/j.solmat.2016.04.017

- When an ASF is built over a glazed building surface, thus including the effects of adaptive shading on the building energy consumption.
- The location of the ASF including the effects of the GWP of the local electricity mix. Assessments will also be run in Madrid and Geneva.
- A static version of the ASF, where panels are optimally orientated at 45° to the horizontal (altitude) axis.
- The type of actuation system (servo motors compared to soft robotic actuators).
- The complexity of the control system. The ASF can be built where each panel is independently actuated, or a case where it is actuated in rows. When the panels are actuated independently more valves and control electronics are required.

3. Results

We present the results of the LCA analysis in relation to the (1) embodied emissions, (2) a calculation of the emission factor, (3) sensitivity of the LCA to design and location, and (4) a comparison to other PV technologies.

3.1. LCA of the adaptive solar facade manufacture

A breakdown of six major midpoint impact indicators based of the ReCiPe methodology [29] can be found in Fig. 6. The largest embodied GWP contribution in the ASF comes from the solar panels, followed by the electronics and the supporting structure. The control and electronics systems play a large role in freshwater eutrophication, and human toxicity due to the high life cycle emissions of electronic systems.

3.2. Calculation of GWP emission factor

The combined GWP of main inputs to the ASF, previously described in Fig. 4, can be illustrated using a waterfall chart as shown in Fig. 7.

This gives us a final emission of 3037 $kgCO_2$-eq. When we include the energy savings through adaptive shading in our system expansion, the final emissions come down to −8318 $kgCO_2$-eq. Dividing these values by the photovoltaic electricity production over a 20 year lifetime of 9175 kWh, we get an emission factor of 331 gCO_2-eq/kWh for the system without adaptive shading and −906 gCO_2-eq/kWh with adaptive shading.

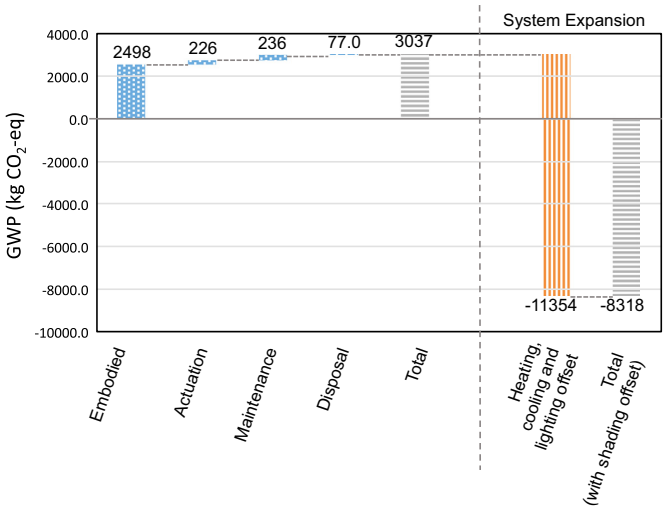

Fig. 7. Waterfall diagram of GWP of the ASF not including photovoltaic electricity production. When reading from left to right, the far left bar details the embodied carbon emissions. The second, third and fourth bar detail the actuation, maintenance, and disposal respectively. This leaves us with our final emissions value (grey bar) of 3037 $kgCO_2$-eq. The orange bar details the emission reduction through adaptive shading which is part of our system expansion bringing the total down to −8318 $kgCO_2$-eq. When we divide these totals by the photovoltaic electricity production (9174 kWh) we gain an emission factor of 331 gCO_2-eq/kWh for the system without adaptive shading and −906 gCO_2-eq/kWh with adaptive shading. Note that the waterfall chart itself does not show PV electricity generation. This is taken into account in the emission factor. (For interpretation of the references to color in this figure caption, the reader is referred to the web version of this paper.)

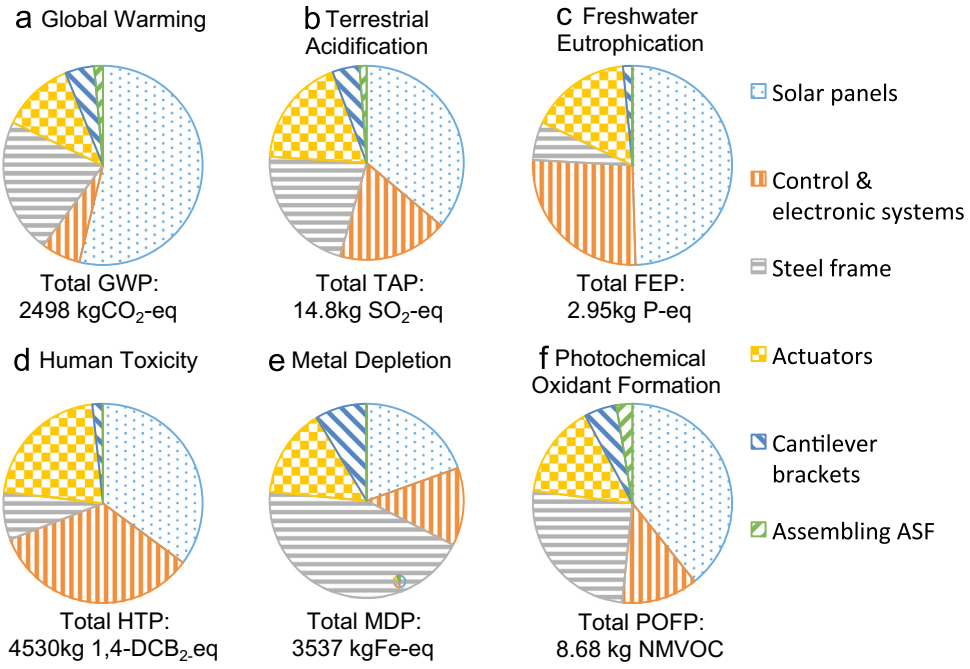

Fig. 6. Embodied emission breakdown of six major midpoint indicators. The solar panels, control/electronics, and steel frame have the highest life cycle impact.

Please cite this article as: P. Jayathissa, et al., Life cycle assessment of dynamic building integrated photovoltaics, Solar Energy Materials and Solar Cells (2016), http://dx.doi.org/10.1016/j.solmat.2016.04.017

3.3. Sensitivity analysis

The sensitivity analysis is shown in Fig. 8. The performance of the ASF is dependent on the location where it is operated as explained in Section 2.2. Changing the weather files of the simulation, and the electricity mix of the country brings interesting results. Geneva has a similar climate to Frankfurt, however the local electricity mix is dominated by hydro and nuclear power which has a very low GWP potential [28]. This would then increase the emission factor of the ASF to 53.5 gCO_2-eq/kWh. This difference arises as the greenhouse gas emission savings of adaptive shading are dependent on the emission factor of the grid mix. Spain on the other hand has a warmer climate, with higher solar radiation, but a less greenhouse gas intensive electricity mix. This ultimately results in a similar emission factor of the ASF of −825 gCO_2-eq/kWh.

We also present a case where we remove the actuators and necessary control system for a dynamic system. Instead, we have panels that are optimally orientated at 45° to the horizontal axis. This reduces embodied greenhouse gas emissions by 12.1% from the baseline highlighted in Fig. 6. However the reduction in electricity production, and savings through adaptive shading, result in a 15% higher emission factor.

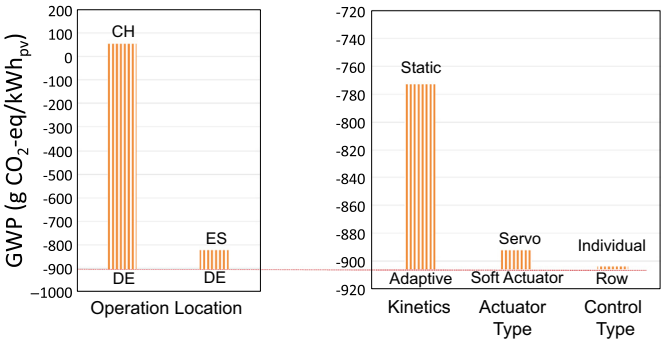

Fig. 8. Sensitivity analysis of the emission factor including the HVAC impact of adaptive shading based on location, actuation system, and control system.

The choice of actuator has a small impact on the embodied carbon emissions. Changing a single Soft Robotic Actuator (including the air compressor, tubing, and maintenance) to a classical servo motor increases the total embodied GWP by 23% from 2498 kg CO_2-eq to 3073 kg CO_2-eq. However, the servo motors have lower operational emissions and maintenance. Ultimately an ASF with servo motors has a 1.5% higher emission factor.

The control system design should be carefully thought out due to the high embodied human toxicity, freshwater eutrophication and terrestrial acidification. However simplifying the actuation control electronics has a minimal effect as the majority of the emissions lie in the inverter, cables, and air compressor. In terms of GWP, there is a 0.3% difference which is negligible.

3.4. Comparison to existing PV technologies

Comparison of the ASF to other PV technologies and the German electricity mix is highlighted in Fig. 9. This comparison is conducted in Frankfurt am Main with an average irradiation of 855 kWh/m^2/year.

The blue bars detail systems with no added shading benefits. Here we present the ASF, a static optimally orientated facade as used in Fig. 8, and three classical flat facade installations. The orange bars detail the system expansion where the ASF is built over glazed surfaces which also bring energy savings to the building. Because the GWP savings through adaptive shading offsets the entire embodied GWP, we have a system with a negative emission factor.

4. Discussion

An adaptive solar facade, purely as a solar tracking and electricity generation technology, is inferior to simple flat mounted static solutions in terms of life cycle emissions. Classic static facade mounted Poly-Si and CIGS solutions perform 40–50% better than the ASF respectively. This is due to the additional greenhouse gas emissions, caused by the material required for the control system, supporting structure, actuators, and the energy required for actuation. A static ASF where the solar panels are orientated for

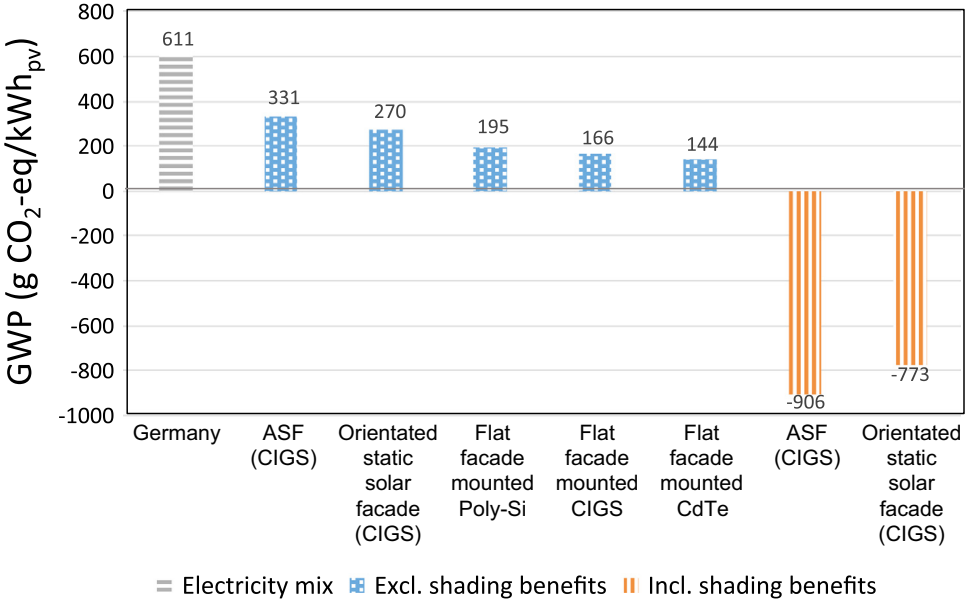

Fig. 9. Comparison of facade installations in Germany with an average facade irradiation of 855 kWh/m^2/year. We compare an ASF to an optimally orientated static facade, and classic flat facade mounted PV solutions. The orange bars include the system expansion of energy savings through adaptive shading. (For interpretation of the references to color in this figure caption, the reader is referred to the web version of this paper.)

Please cite this article as: P. Jayathissa, et al., Life cycle assessment of dynamic building integrated photovoltaics, Solar Energy Materials and Solar Cells (2016), http://dx.doi.org/10.1016/j.solmat.2016.04.017

optimal harvest also has a lower life cycle performance compared to classic facade systems. This is because the added structure required for optimal orientation is not compensated by the added gains in photovoltaic production.

However when we also consider the multi functionality of the ASF and account for energy savings to the building through adaptive shading, we have a system that yields a negative emission factor of -906 gCO_2-eq/kWh. This is because the savings to the building system in terms of heating, cooling, and lighting offsets the embodied GWP four-fold. This demonstrates the advantage of using the PV material, not only as an electricity generation unit, but also as a building material for adaptive shading systems. In this analysis we also present a static ASF where all panels were orientated at an optimal angle of 45° to the horizontal axis. Although this solution performs well, it sacrifices user comfort. The users cannot open the facade to suit their desires.

GWP savings through adaptive shading however are sensitive to the GWP of the electricity mix. A country with a low GWP electricity mix will result in lower operational GWP savings than a country with a high GWP electricity mix. For example, an ASF installed in Switzerland has a higher emission factor of 53.5 gCO_2-eq/kWh.

Although it is favourable to install an ASF in Germany, it still has benefits in countries such as Switzerland. For instance, with an emission factor 53% less than the standard mix, it contributes to a nuclear free energy mix. Furthermore, it provides interesting design options for architects where they can install PV in locations which were previously not possible. Thus increasing BIPV potential.

When designing an ASF architects and engineers may consider:

- The added benefit of a highly adaptable shading element.
- The trade-off between soft robotic actuators and servo motors for actuation. Although the investigated soft robotic actuator has an embodied GWP three times lower than a servo motor, it requires three times more energy to actuate. Purely from an LCA perspective, if more than 6 actuations are required a day, servo motors would be the preferred solution.
- Control system electronics cost 27.5 $kgCO_2$-eq/kg and play a large contribution in human toxicity, freshwater eutriphication and terrestrial acidification. They should therefore be carefully designed. However increasing the resolution of the ASF control system to allow each panel to be independently actuated only increases the emission factor by 1.6 gCO_2-eq/kWh.
- The structural support system in our current analysis used a stainless steel frame representing 22% of our total embodied carbon emissions, 21% of terrestrial acidification, 44% of metal depletion, and 25% of photochemical oxidant formation. Redesigning the frame to use less stainless steel, or an alternative material with a lower life cycle impact, such as plain steel, should be considered.
- If the ASF is installed in front of an opaque building surface then the advantages of adaptive shading are not present. In this case, a static, flat mounted system is a preferred design choice.

One limitation of the LCA is that the analysis focuses on a single office room. Expanding the analysis to the entire building, or urban level may yield different results. The LCA also assumes that the user will not override the system. In practice the facade will adapt to the desires of the user. The LCA also excludes other aspects of building system such as the downsizing of heating and cooling appliances, the use of DC electricity on-site, and the increase in user comfort.

5. Conclusion

As an electricity producing device the ASF is outperformed by fixed PV systems. However it comes with the added benefit of building integration and multifunctionality, i.e. allowing for better control of solar loads and user comfort. When adding these aspects to the comparison (i.e. accounting for HVAC savings), the system becomes favourably competitive to a traditional PV system as it has a negative emission factor of -906 gCO_2/kWh. These advantages however, will not be present if the ASF is installed over an opaque building surface. It is therefore preferable to install static systems over opaque facades, and keep the adaptive system for glazed facades only.

The design of an ASF can greatly influence the results. Varying factors such as the choice of actuators, the complexity of the control system, and the structural support can change the emission factor. The largest variable however is the emission factor of the grid electricity mix. The building operational savings in heating, cooling, and lighting will have a CO_2 saving based on the grid electricity mix.

Future research will validate the assumptions to building energy consumption through experimentation, and test the users response. This will be conducted on the ETH House of Natural Resources living lab where an example of an ASF has already been constructed [11]. Further numerical simulations of the ASF on different building typologies, building systems and climates will enable us to specifically target the best application scenario.

To conclude, we demonstrated that BIPV systems and adaptive shading elements complement each other successfully. We see an improvement in environmental performance of the PV technology, and create new architectural possibilities for the aesthetic integration of PV panels over glazed building surfaces, thus expanding BIPV potential.

Acknowledgements

The authors would like to acknowledge the HiLo and HoNR project members for the design and construction of the ASF: Supermanoeuvre (Sydney Australia) and the Professorship of Architecture and Structures (BRG, ETH Zurich) for their work in designing the HiLo building; and the Institute of Structural Engineering (IBK, ETH Zurich) for their work in designing the HoNR building. We would also like to thank Professor Stefanie Hellweg for her support in the LCA analysis. The authors would also like to thank other key contributors to the ASF Project: Bratislav Svetozarevic, Moritz Begle, Johannes Hofer, Nicola Offeddu, Giovanni Bianchi, and Jeremias Schmidli.

This research was partly funded by the Climate-KIC, Building Technologies Accelerator program.

Appendix A

A.1. Electricity production of different PV systems

See Table 8.

Table 8
Total PV production for the ASF, a static version of the ASF in an optimal orientation for building shading and PV production, and classical flat facade mounts of CIGS, CdTe and PolySi panels in Frankfurt, Germany.

	ASF	Orientated solar facade	Flat CIGS	Flat CdTe	Flat PolySi
Total irradiation (kWh/m^2/year)	855.0	855.0	855.0	855.0	855.0
Utility factor (m^2/m^2)	0.69	0.69	0.69	0.69	0.69
Losses from sub optimal angle	0.00	0.30	0.38	0.38	0.38
Irradiation of active PV (kWh/m^2/year)	593.8	415.6	365.3	365.3	365.3
Efficiency	0.11	0.11	0.11	0.10	0.14
Self shading losses	0.40	0.40	0.00	0.00	0.00
Losses due to sub optimal tracking angle	0.77	1.00	1.00	1.00	1.00
Total power (kWh/year)	458.7	417.0	610.8	555.3	777.4

A.2. Major contributions to disposal

See Table 9.

Table 9
Major disposal global warming potential (GWP) and terrestrial acidification potential (TAP) contributions to the disposal of an ASF. Note that the cut off system model is used.

Disposal Contribution	GWP	TAP
Treatment of waste polyurethane, municipal incineration	32.7	0.0223
Treatment of waste electric wiring, collection for final disposal	31.6	0.0162
Treatment of scrap aluminium, municipal incineration	3.93	0.0404
Treatment of scrap steel, municipal incineration	3.7	0.039
Treatment of electronics scrap from control units	2.89	0.001
Treatment of waste polyethylene, municipal incineration	1.07	0.0001
Market for waste electric, and electronic equipment	0.923	0.00178
Treatment of scrap copper, municipal incineration	0.285	0.00051

References

[1] Fifth Assessment Report, Mitigation of Climate Change, Intergovernmental Panel on Climate Change, pp. 674–738.
[2] P. Defaix, W. van Sark, E. Worrell, E. de Visser, Technical potential for photovoltaics on buildings in the EU-27, Sol. Energy 86 (9) (2012) 2644–2653.
[3] M. Raugei, P. Frankl, Life cycle impacts and costs of photovoltaic systems: current state of the art and future outlooks, Energy 34 (3) (2009) 392–399.
[4] G. Wilson, Cell efficiency records ⟨http://www.nrel.gov/ncpv/⟩, 2015.
[5] K. Kushiya, CIS-based thin-film PV technology in solar frontier KK, Sol. Energy Mater. Sol. Cells 122 (2014) 309–313.
[6] M. Kaelin, D. Rudmann, A. Tiwari, Low cost processing of CIGS thin film solar cells, Sol. Energy 77 (6) (2004) 749–756.
[7] B.P. Jelle, C. Breivik, H.D. Røkenes, Building integrated photovoltaic products: a state-of-the-art review and future research opportunities, Sol. Energy Mater. Sol. Cells 100 (2012) 69–96.
[8] D. Rossi, Z. Nagy, A. Schlueter, Adaptive distributed robotics for environmental performance, occupant comfort and architectural expression, Int. J. Archit. Comput. 10 (3) (2012) 341–360.
[9] R. Loonen, M. Trčka, D. Cóstola, J. Hensen, Climate adaptive building shells: state-of-the-art and future challenges, Renew. Sustain. Energy Rev. 25 (2013) 483–493.
[10] P. Jayathissa, Z. Nagy, N. Offedu, A. Schlueter, Numerical simulation of energy performance and construction of the adaptive solar facade, Proc. Adv. Build. Skins 2 (2015) 52–62.
[11] Z. Nagy, B. Svetozarevic, P. Jayathissa, M. Begle, J. Hofer, G. Lydon, A. Willmann, A. Schlueter, The adaptive solar facade: From concept to prototypes, Front. Archit. Res., http://dx.doi.org/10.1016/j.foar.2016.03.002.
[12] M. Raugei, S. Bargigli, S. Ulgiati, Life cycle assessment and energy pay-back time of advanced photovoltaic modules: cdTe and CIS compared to Poly-Si, Energy 32 (8) (2007) 1310–1318.
[13] M.M. de Wild-Scholten, Energy payback time and carbon footprint of commercial photovoltaic systems, Sol. Energy Mater. Sol. Cells 119 (2013) 296–305.
[14] V. Fthenakis, H.C. Kim, Photovoltaics: life-cycle analyses, Sol. Energy 85 (8) (2011) 1609–1628.
[15] J. Mason, V. Fthenakis, T. Hansen, H. Kim, Energy payback and life-cycle co2 emissions of the BOS in an optimized 3 · 5 MW PV installation, Prog. Photovolt.: Res. Appl. 14 (2) (2006) 179–190.
[16] M. Finkbeiner, A. Inaba, R. Tan, K. Christiansen, H.-J. Klüppel, The new international standards for life cycle assessment: ISO 14040 and ISO 14044, Int. J. Life Cycle Assess. 11 (2) (2006) 80–85.
[17] O. Ortiz, F. Castells, G. Sonnemann, Sustainability in the construction industry: a review of recent developments based on LCA, Constr. Build. Mater. 23 (1) (2009) 28–39.
[18] R. Frischknecht, N. Jungbluth, H.-J. Althaus, G. Doka, R. Dones, T. Heck, S. Hellweg, R. Hischier, T. Nemecek, G. Rebitzer, et al., The ecoinvent database: overview and methodological framework (7 pp), Int. J. Life Cycle Assess. 10 (1) (2005) 3–9.
[19] S. Solomon, Climate Change 2007—The Physical Science Basis: Working Group I Contribution to the Fourth Assessment Report of the IPCC, vol. 4, Cambridge University Press, 2007.
[20] A. Ciroth, ICT for environment in life cycle applications openLCA new open source software for life cycle assessment, Int. J. Life Cycle Assess. 12 (4) (2007) 209–210.
[21] A. Chirilă, S. Buecheler, F. Pianezzi, P. Bloesch, C. Gretener, A.R. Uhl, C. Fella, L. Kranz, J. Perrenoud, S. Seyrling, et al., Highly efficient Cu (In, Ga) Se2 solar cells grown on flexible polymer films, Nat. Mater. 10 (11) (2011) 857–861.
[22] B. Svetozarevic, Z. Nagy, D. Rossi, A. Schlueter, Experimental Characterization of a 2-DOF Soft Robotic Platform for Architectural Applications, Robotics: Science and Systems, Workshop on Advances on Soft Robotics, 2014, pp. 2–6.
[23] Rhinoceros v5 ⟨https://www.rhino3d.com/⟩, 2015.
[24] Grasshopper—algorithmic modeling for rhino ⟨http://www.grasshopper3d.com/⟩, 2015.
[25] D.B. Crawley, L.K. Lawrie, C.O. Pedersen, F.C. Winkelmann, Energy plus: energy simulation program, ASHRAE J. 42 (4) (2000) 49–56.
[26] Diva for rhino ⟨http://diva4rhino.com/⟩.
[27] MATLAB 2014b, The MathWorks, Inc., Natick, Massachusetts, United States.
[28] R. Itten, R. Frischknecht, M. Stucki, Life Cycle Inventories of Electricity Mixes and Grid, 2012.
[29] M. Goedkoop, R. Heijungs, M. Huijbregts, A. De Schryver, J. Struijs, R. van Zelm, ReCiPe 2008, A Life Cycle Impact Assessment Method Which Comprises Harmonised Category Indicators at the Midpoint and the Endpoint Level 1.

Please cite this article as: P. Jayathissa, et al., Life cycle assessment of dynamic building integrated photovoltaics, Solar Energy Materials and Solar Cells (2016), http://dx.doi.org/10.1016/j.solmat.2016.04.017